Unsteadiness of the Separation Shock Wave Structure in a Supersonic Compression Ramp Flowfield

D. S. Dolling* and M. T. Murphy†
Princeton University, Princeton, New Jersey

Wall pressure fluctuations have been measured in a two-dimensional separated compression ramp-induced shock wave turbulent boundary-layer interaction. The tests were made at a nominal freestream Mach number of 3 and at Reynolds numbers based on boundary-layer thickness of 7.8×10^5 and 1.4×10^6. The wall temperature condition was approximately adiabatic. Large-amplitude pressure fluctuations exist throughout the interaction, particularly near separation and reattachment. In the upstream region of the flowfield, the unsteadiness of the separation shock wave structure generates an intermittent wall pressure signal. Mean wall pressures in this region result from the superposition of the relatively low-frequency, large-amplitude, shock wave-induced fluctuations on the pressure signal of the undisturbed boundary layer. This behavior is qualitatively similar to that observed in three-dimensional blunt fin-induced flows. In these two flowfields, the length scale of the shock motion is a significant fraction of the distance from the interaction start to separation.

Nomenclature

D = blunt fin leading-edge diameter
f = frequency, Hz
L_i = streamwise length of intermittent region
L_{sep} = time averaged separated flow length
L_u = upstream influence
M = Mach number
n = number of data points used in calculating $\bar{P}$, etc.
N = number of data records
N_L = crossings per second of a given pressure level
q = dynamic pressure
P = instantaneous static pressure
$\bar{P}$ = mean static pressure $= \frac{1}{n}\sum_{i=1}^{n} P_i$
Re = Reynolds number $(U_\infty/\nu_\infty)m^{-1}$
U = velocity
X = streamwise distance from ramp corner
α_j = skewness ($j=3$) and kurtosis ($j=4$) coefficients
$= \dfrac{\frac{1}{n}\sum_{i=1}^{n}(P_{wi}-\bar{P}_w)^j}{\sigma p_w^j}$
γ = intermittency, Eq. (1)
δ = boundary-layer thickness
ν = kinematic viscosity
σp_w = wall pressure standard deviation
$= \left[\sum_{i=1}^{n}(P_{wi}-\bar{P}_w)^2/n-1\right]^{1/2}$
τ = shear stress

Subscripts

∞ = based on incoming freestream conditions
0 = measured just upstream of interaction
w = measured at the wall

Received May 27, 1982; presented as Paper 82-0986 at the AIAA/ASME Third Joint Thermophysics, Fluids, Plasma and Heat Transfer Conference, St. Louis, Mo., June 7-11, 1982; revision received Dec. 13, 1982.

*Research Staff Member and Lecturer, Dept. of Mechanical and Aerospace Engineering. Now Assistant Professor at University of Texas. Member AIAA.

†Graduate Student, Dept. of Mechanical and Aerospace Engineering. Member AIAA.

Introduction

In recent years, substantial progress has been made in computational fluid dynamics. One of the most challenging problems facing the field is the simulation of shock wave-induced turbulent boundary-layer separation. Such flows incorporate all of the difficulties of compressibility, turbulence, and viscous-inviscid interaction and, in practice, are usually three-dimensional. Despite the difficulties, codes have been developed which, with differing degrees of quantitative success, can capture many of the features of a range of two- and three-dimensional (2-D, 3-D) interactive flows (e.g., Refs. 1-3).

To maintain progress, the capabilities and limitations of such computer codes must be investigated, and the reasons for their successes and failures identified. Doing this will require a much better understanding of interactive flows than exists at present. Currently, drawing meaningful conclusions from comparisons of numerical predictions with experimental data can be difficult, particularly in cases where the underlying physics which generate the particular experimental result are not well understood. In interpreting experimental data, a critical element is flowfield unsteadiness. In this context, unsteady flows are considered as being those in which there are significant variations in either the structure or scale, or both, of parts or all of the flowfield. Since the majority of experimental data consists of time-averaged measurements, such as wall pressures measured using surface orifices or velocity profiles deduced from pitot-static surveys, there is little quantitative information on the steadiness of many interactive flows.

A common feature in the available data set, which dates back to the 1950s, is the relatively large-scale unsteadiness of the separation process. In forward facing step flows, random shock motion with a length scale of ⅓ to ½ of the boundary-layer thickness δ_0 has been observed.[4] Kistler[5] has shown that the wall pressure signal near separation in such flows can be modeled as a step function, with the jump location (i.e., the shock wave) moving over some range. Similar results have been obtained in 3-D flows, notably in those induced by blunt fins and cylindrical protuberances, at transonic and super-

sonic speeds.[6-11] In these cases, high-speed photography and wall pressure fluctuation measurements have shown that large variations occur in the position and structure of the separation shock wave system. At hypersonic speed (Mach 7) in an interaction generated by a flare mounted concentrically on a cone-ogive-cylinder model, large-scale unsteadiness of the separation onset and reattachment regions has been observed.[12] From measured convection velocities and the peak frequency, the scale was estimated to be of order the length of the separated region. In other separated flows[13,14] in which wall pressure fluctuations were measured, distributions of the standard deviation, σ_{p_w}, near separation are qualitatively and quantitatively similar to those in Refs. 5 and 11, suggesting that the separation shock wave structure is similarly unsteady.

These results have prompted a re-examination of a 2-D, separated compression, ramp-induced interaction, whose flowfield and surface properties were obtained using time-averaged techniques in earlier studies.[15,16] In the new test program, carried out in the same wind tunnel and at the same freestream conditions, wall pressure fluctuations have been measured along a streamwise cut through the interaction. Results from the study are presented in this paper. The primary focus is on the properties of the unsteady separation shock wave structure.

Experimental Techniques

Wind Tunnel and Model

All tests were made in the Princeton University 20×20 cm high Reynolds number blowdown tunnel. The model was mounted on the tunnel floor at approximately 16 cm (station 1) and 107 cm (station 2) downstream of the nozzle exit plane. At these stations, M_∞ is uniform and equal to 2.95 and 2.90, respectively. The stagnation pressure for all tests was 6.8×10^5 Nm$^{-2}\pm1\%$ and the stagnation temperature was 265 K$\pm5\%$ giving a nominal freestream Reynolds number of 6.5×10^7 m^{-1}. The wall temperature was approximately adiabatic.

In designing the model (Fig. 1), the main objective was to obtain a 2-D flowfield. Two 24 deg solid brass, 15-cm-long ramps were used. Both were 15 cm wide, allowing a 2.5 cm gap on either side for passage of the sidewall boundary layers. To isolate the interaction further and prevent spillage out of the separated flow region, side fences were used. They had the same shape and size as used earlier,[16] and had evolved out of a parametric study of fence geometries and their effects on the flowfield. With these fences, transverse pressure distributions were uniform and end effects were small. Surface streak patterns, which are extremely sensitive to spanwise nonuniformities, show that the flow is essentially two-dimensional. Minor 3-D perturbations occur in the separation region, causing a slight waviness in the separation line, but their influence is small. The spanwise variation in the length of the separated flow is only a few percent.

Measurements upstream of the corner were made using a flush pressure transducer in a wall plug. The ramp was moved relative to the transducer. Over the range of travel ($\sim$6 cm), the change in δ_0 of approximately 0.06 cm has a negligible effect on the flowfield. At each position, the ramp was clamped to the floor and sealed with rubber cement. Measurements on the ramp face were made with a second model which could be slid 1.25 cm into or out of the tunnel floor along the plane of the face. The transducer was installed in one of five plugs in the face. They were centered 2.54 cm apart and were flush with the surface to within ±0.0001 cm. Thus, measurements could be made anywhere in the range $0\le X\le+13$ cm. Tests made using adjacent plugs, but at the same X, showed no effect of ramp length changes.

Instrumentation

Wall pressures were measured using a Kulite differential transducer (Model XCQ-062-25-D) referenced to vacuum. It has a 0.071-cm-diam silicon diaphragm in which a fully active Wheatstone bridge has been bonded atomically. The natural frequency is $\sim$500 kHz. It was calibrated statically. Shock tube tests have shown that transducers of this type have dynamic calibrations only a few percent lower than those obtained statically.[17] The transducer signal was amplified, filtered, and sampled digitally at 500 kHz. Data were taken in files of N records, each consisting of 1024 pressure measurements. The value of N necessary for convergence of $\bar{P}_w$, σp_w, and the higher order moments depends on the signal characteristics and is therefore a function of position. Values in the range $100\le N\le900$ ensured convergence at all positions.

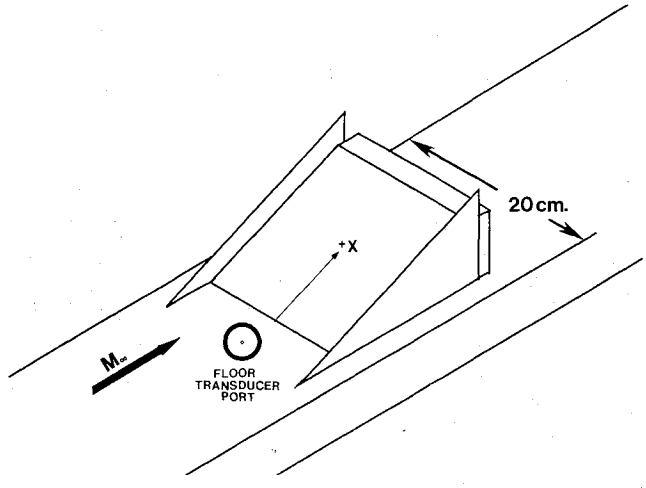

Fig. 1 Model and coordinate system.

STATION	δ_{CM}	δ^*_{CM}	θ_{CM}	C_f	$R_{E\theta}$	π
1 □	1.25	0.32	0.064	0.00119	38,600	.574
2 △	2.21	0.56	0.113	0.00108	69,100	.614

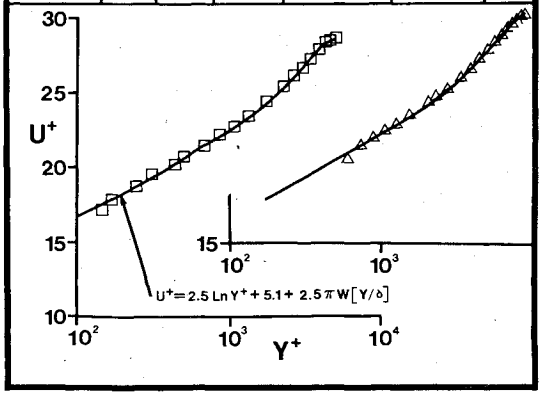

Fig. 2 Incoming mean velocity profiles.

Incoming Boundary Layers

Figure 2 shows the incoming mean velocity profiles plotted in wall coordinates u^+ vs y^+. At both stations the profiles match the wall-wake law well. The skin-friction coefficients agree well with values predicted by the Van Driest II theory, and the values of the wake strength parameter (Λ) are in the normal range for equilibrium turbulent boundary layers. Trips were not used since at such high Reynolds numbers transition occurs far upstream of the nozzle exit.

Wall pressure fluctuations under attached, zero-pressure gradient, turbulent boundary layers have been studied by many investigators over a wide range of conditions. At high speeds, broadband quantities such as σp_w have been reasonably well correlated by plotting $\sigma p_w/q_\infty$ (or with less

success, $\sigma p_w/\tau_w$) against M_∞.[14,18] Considerable scatter exists, but the trend is that σ_{pw}/q_∞ decreases with increasing M_∞. The present tests give $\sigma p_w/q_\infty = 2.6\times10^{-3}$ ($\sigma p_w/\tau_w = 2.2$), which agree well with the correlated data in Refs. 14 and 18. Normalized probability density distributions are essentially Gaussian with a skewness coefficient $\alpha_3 = 0.036 \pm 0.01$ and kurtosis coefficient $\alpha_4 = 2.92 \pm 0.02$. Theoretical values are 0 and 3, respectively. The normalized power spectrum falls in the bands obtained by Lewis[19] at $M_\infty = 2.5$, and by Bies,[20] who correlated data from many studies in the range $0.03 \le M_\infty \le 3.96$.

Results and Discussion

Mean Flowfield and Wall Pressure Distribution

The microsecond spark shadowgram in Fig. 3a shows the characteristic wave pattern of ramp-induced separated flow. In Ref. 16 several spark shadow and continuous light photographs revealed only minor variations in this pattern. Thus, it was assumed that the flowfield was essentially steady. However, unless the separation shock wave motion was uniform across the width of the interaction, it would not be detectable from photographs. Since the technique averages across the flowfield, random spanwise variations in position (which flow visualization suggests is the case[21]) would result in essentially the same image from frame to frame.

Figure 3b shows the mean flowfield model deduced from pitot and static pressure surveys.[16] Mean wall pressures have been measured in many studies and the general features are well known. The results obtained using the Kulite transducer are shown in Fig. 4a. The separation and reattachment points indicated by S and R were determined from kerosene-lampblack surface flow patterns. In the following discussion it is these points that are implied when the terms separation and reattachment are used. In Ref. 16, $\bar{P}_w$ was measured using surface orifices and a scanivalve. The data agree well with Fig. 4a, although the latter have slightly higher levels throughout, and match the theoretical downstream pressure level more closely.

Distributions of the Wall Pressure Standard Deviation

Figure 4b shows the corresponding distributions of σp_w normalized by $\bar{P}_w$. The data correlate well at the two stations. Both distributions have two peaks, one upstream of separation, the other at, or extremely close to, reattachment. In the region where the upstream peak in σp_w occurs, the wall pressure signal and its statistical properties are qualitatively similar to those at the same relative position in blunt fin-induced flows.[11] Both have the features characteristic of an unsteady shock wave structure. In the blunt fin flow, independent confirmation of the unsteadiness and the streamwise scale of the motion were obtained from high-speed photography.[10] In the present tests, only wall pressures were measured, but these are sufficient to quantify the unsteadiness.

From separation to the corner, σp_w and $\bar{P}_w$ both increase but their ratio is approximately constant. In absolute terms, σp_w is about 10 σp_{w_0}, although normalizing by $\bar{P}_w$ halves this factor. The higher-order moments, α_3 and α_4, are plotted in Fig. 5. They also correlate well showing that at the same normalized station the details of the fluctuations are the same. In the separated flow, the distribution is almost Gaussian,

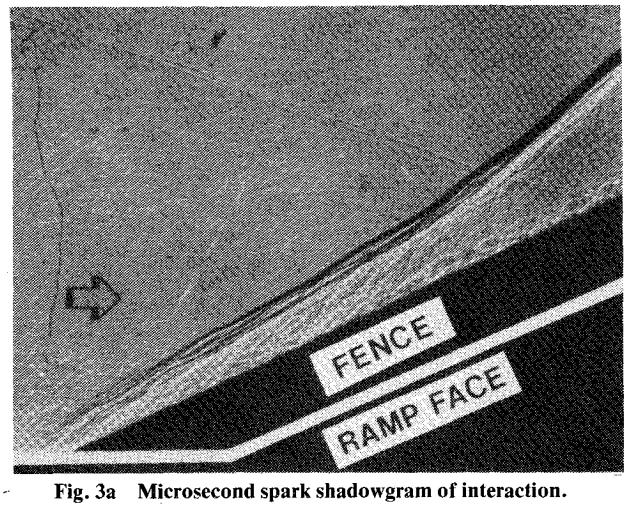

Fig. 3a Microsecond spark shadowgram of interaction.

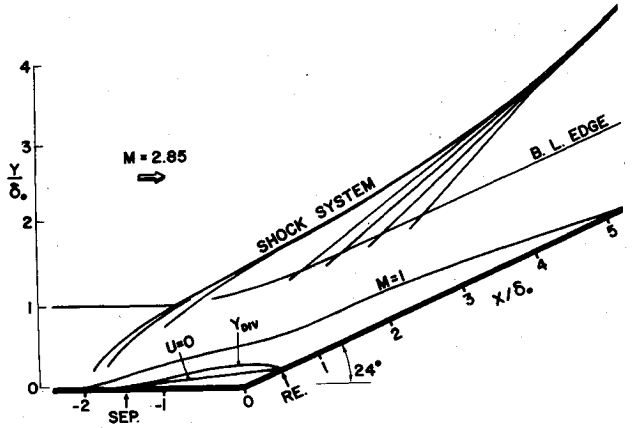

Fig. 3b Experimental mean flowfield model (from Ref. 15).

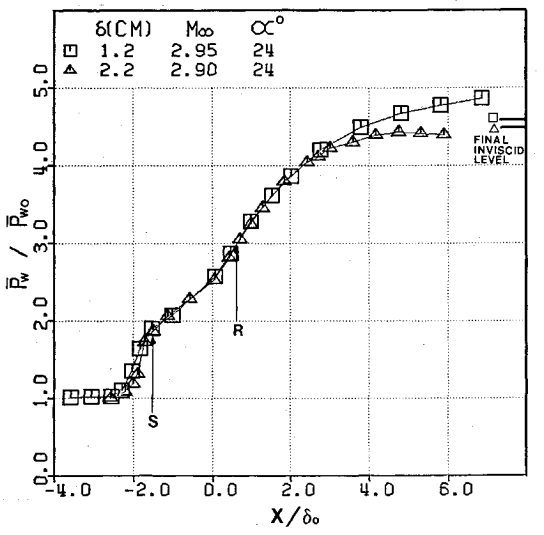

Fig. 4a Mean wall pressure distributions.

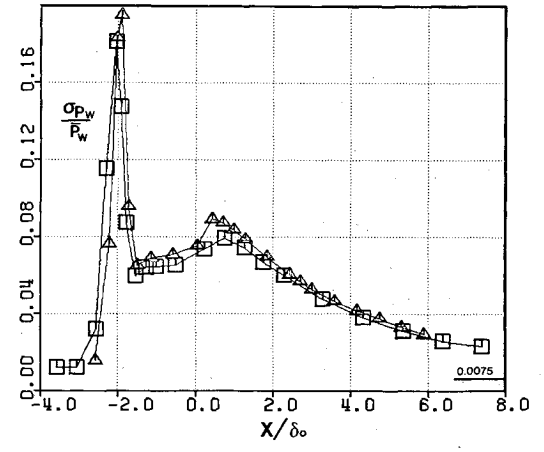

Fig. 4b Wall pressure standard deviation distributions.

becoming more skewed and peaked toward reattachment. The ratio $\sigma p_w/q_\infty$ just downstream of separation is 0.022. In larger scale separated flows generated by 2-D forward facing steps and large-angle flares, $\sigma p_w/q_\infty$ has been found to be approximately constant, increasing rapidly near reattachment.[13,14] In the step flows, values between 0.03 and 0.04 were measured over the range $1.7 \leq M_\infty \leq 3.5$. The underlying trend is that of increasing intensity with increasing M_∞. In the flare tests, $\sigma p_w/q_\infty$ varied from 0.016 at $M_\infty = 1.6$ to 0.023 at $M_\infty = 2.5$.

Downstream of the corner, $\bar{P}_w$ and σp_w increase, with $\sigma p_w/\bar{P}_w$ reaching a maximum near reattachment. The maximum value of σp_w is further downstream but within 1 δ_0 of reattachment. Assuming that the redeveloping boundary layer is approaching an equilibrium state corresponding to the new freestream conditions, then the attached boundary-layer correlation of Ref. 18 would predict $\sigma p_w/\bar{P}_w$ to be 0.007-0.008, as indicated in the figure. An approximate linear extrapolation of the data shows that this would occur at X/δ_0 of about 20.

Flowfield Near Separation

The rapid rise of $\sigma p_w/\bar{P}_w$ upstream of separation appears to be a common feature of many 2-D and 3-D shock wave-induced turbulent separated flows. The relative amplitude of the fluctuations in this region is extremely large, with the maximum value of σp_w being a significant fraction of $\bar{P}_w$. However, this region differs from others not just because of the relative amplitude of the fluctuations but on account of its physical character. It is dominated by the unsteady separation shock wave and the flowfield physics must be interpreted within this framework.

Near the upstream boundary of the flowfield, α_3 and α_4 increase rapidly, reach large maxima, decrease, and then return to approximate Gaussian values near separation. The physical cause is the shock wave motion. This can be seen in pressure-time plots. Two examples, at $X/\delta_0 = -2.1$ and -2.3 are shown in Fig. 6. On each plot, $\bar{P}_w$ is indicated. For reference, the incoming boundary-layer wall pressure signature is also shown. Similar to Kistler's results the instantaneous wall pressure is intermittent, jumping randomly back and forth from the range characteristic of the undisturbed boundary layer to a higher level that varies with shock strength. $\bar{P}_w$ is generated by the superposition of very large amplitude fluctuations on the undisturbed pressure signal and increases in the downstream direction because the fluctuations increase in amplitude and frequency.

Kistler's sketches of the pressure signal, based on oscilloscope traces, suggest an approximately constant disturbance pressure level, while those of the present tests and Ref. 11 show a wide range of values. The maximum value of $\sigma p_w/\sigma p_{w0}$ measured by Kistler was about 16, the same as in the present test. In blunt fin flows, the maximum varied with D and δ_0, and was in the range 15-35. In other studies, the character of the pressure signal was not discussed. Only distributions of σp_w were presented. They all have the same shape as seen in Fig. 4b.

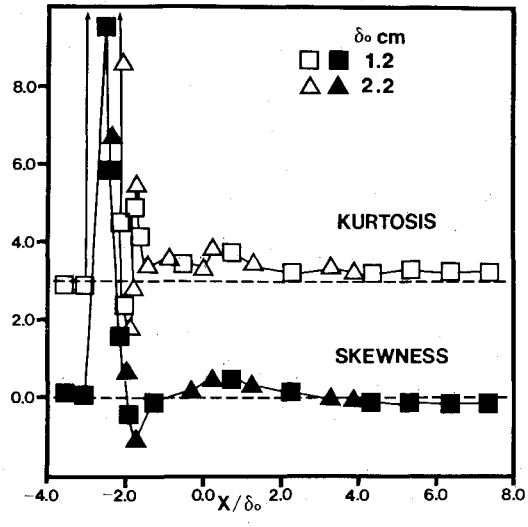

Fig. 5 Skewness and kurtosis distributions.

These results suggest that many of the wall pressure distributions reported in the literature are also time-averaged values of a similar unsteady pressure field. If so, then the dynamic character of many flows has been entirely obscured. In this region, any quantity based on the entire pressure signal is an average value of two distinct superposed signals, and provides little information on the physical properties of either. For example, at $X/\delta_0 = -2.3$, the wall pressure is undisturbed for about 80% of the time, during which $\bar{P}_w = \bar{P}_{w0}$ and $\sigma p_w = \sigma p_{w0}$. The large-amplitude disturbances for the other 20% of the time make $\bar{P}_w$ for the entire signal equal to 1.08 $\bar{P}_{w0}$. Thus, that fraction of the signal representing the undisturbed boundary layer is all below the mean value of the entire signal and it is this, combined with the contribution from the fewer points far above the mean value, that increases σp_w by a factor of 10.

Intermittent Region

At each position an "intermittency" factor, γ, can be calculated. It defines the fraction of time that the flowfield is disturbed. In this context, disturbed means that P_w is outside the range of the undisturbed boundary layer, that is,

$$\gamma = \frac{\text{time}[P_w > (\bar{P}_{w0} + 3\sigma p_{w0})]}{\text{total time}} \tag{1}$$

Based on 100 data records, γ for the incoming boundary layer was 0.0016 compared to 0.0013 for a theoretical Gaussian distribution. The region over which γ increases from some value slightly larger than this to 1 defines the streamwise length scale of the shock structure motion. Figure 7 shows that a large fraction of the region upstream of separation is intermittent. Both curves have the same shape and are displaced from one another due to the change in interaction scale with δ_0. The shape is similar to the Gaussian probability distribution function, but it not quite symmetric about $\gamma = 0.5$. The measured curves have longer and shorter tails for low and high γ, respectively. The upstream tails decrease gradually toward $\gamma = 0.0016$, such that the absolute length of the intermittent region, L_i, is about 0.75-0.9 δ_0. Pressure-time histories show disturbances at these upstream stations, but the combination of small γ and low strength does not generate a measurable increment in $\bar{P}_w$. Since long sampling times are needed to define γ accurately when it is less than about 0.02 to 0.03, a more accurate comparision of the two cases can be made by defining L_i as the distance over which γ increases from about 0.04 to 0.99. This gives 0.6 δ_0 in both cases and represents the region over which $\bar{P}_w/\bar{P}_{w0}$ increases from about 1.03 to about 1.7.

No direct measurements could be made of the instantaneous separation point motion. When surface streak patterns were obtained starting with the kerosene-lampblack mixture painted only along the corner line, a well-defined line (the separation line) was formed upstream. Close examination of the line shows that many variable length streaks project forward of it and are records of instants when the reversed flow extended further upstream. This suggests that the separation line indicated by this technique may represent the downstream boundary of a band of separation. The existence of such a band, and a ragged instantaneous spanwise separation line, have been qualitatively confirmed by flow visualization,[21] but there are no quantitative data on its length scale or properties.

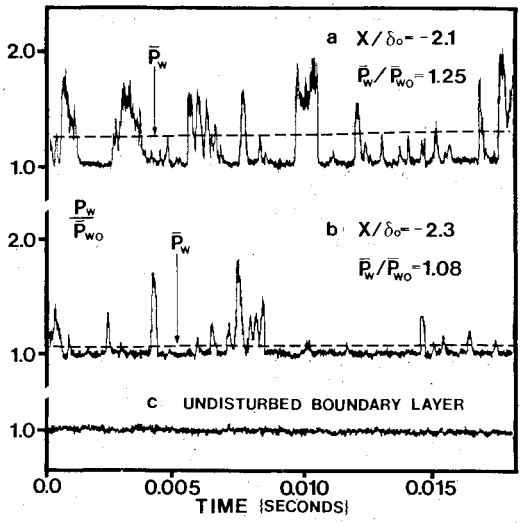

Fig. 6 Pressure-time histories near separation.

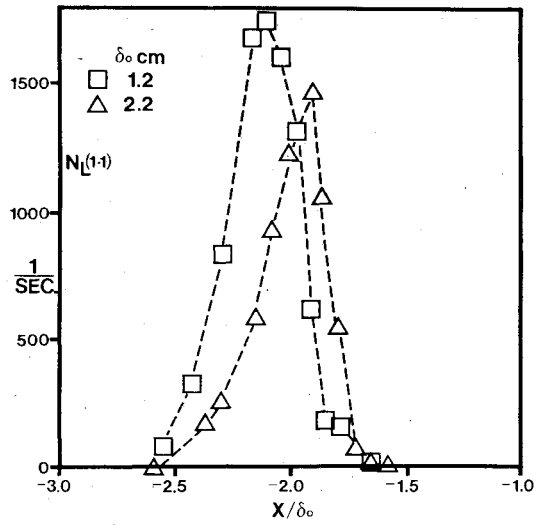

Fig. 8 Shock motion frequency in intermittent region.

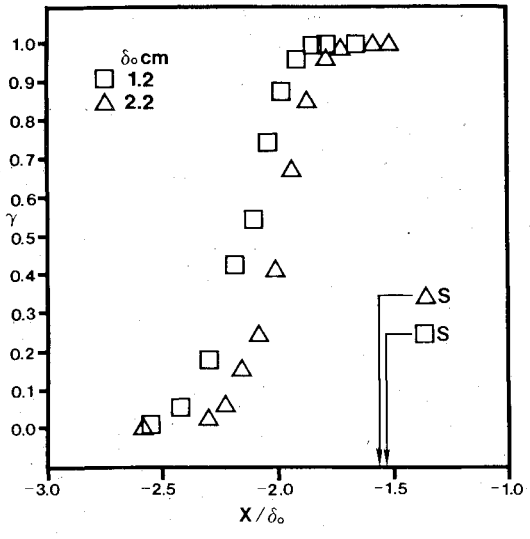

Fig. 7 Streamwise distributions of γ.

Intermittent Region Length Scale

Intermittency also occurs in semi-infinite blunt fin-induced flows. In Ref. 11 tests were made using two different diameter leading edges ($D=1.27$ and 2.54 cm) in two turbulent boundary layers ($\delta_0=0.3$ and 1.6 cm). The freestream and wall temperature conditions were the same as in the current tests. The intermittency curves had the same shape as those in Fig. 7 and occupied the same relative region of the flowfield. L_i normalized by D fell in the narrow range $0.42 \leq L_i/D \leq 0.54$, whereas in terms of δ_0 it varied from 0.4 δ_0 to 3.4 δ_0. This contrasts with the compression ramp data which, although limited to only two test conditions, suggest that δ_0 is the appropriate scaling parameter for L_i.

A later test program, in which wall pressure fluctuations were measured upstream of the corner for different ramp angles has shown that the common feature with the blunt fin flows is that L_i occupies a significant fraction of the distance from the interaction start to separation. These results are reported in Ref. 22.

Shock Motion Frequency

No periodicity was detectable in the wall pressure signal. Energy spectra show that, compared to the undisturbed boundary-layer signal, there is significant amplification at frequencies less than about 10 kHz, but the distribution is broadband. An alternative method of presenting frequency information, which is useful for comparative purposes, is to determine the number of crossings per second, $N_L(P_L)$, of a given pressure level, P_L. If P_L is set equal to 1.1 P_{w0}, then it is high enough to exclude the undisturbed boundary-layer fluctuations but low enough to include those induced by relatively weak shock waves. Thus, although $N_L(1.1)$ does not represent the frequency of a given strength disturbance, it is a measure of the maximum frequency at which the wall pressure is increased above the undisturbed level. In processing the data records, the counter registering N_L was inactive after each crossing until the wall pressure was again within the undisturbed range [i.e., $P_w < (\bar{P}_{w0} + 3\sigma p_{w0})$]. This ensured that the large-amplitude fluctuations occurring when the shock wave is upstream of the transducer were not included in N_L.

Distributions of $N_L(1.1)$ vs X/δ_0 are shown in Fig. 8. The maximum values at stations 1 and 2 are in the range 1.8-1.9 kHz and 1.4-1.5 kHz, respectively. L_{sep}/δ_0 is about 2.1 in both cases, although at station 2, δ_0 is larger. L_{sep} is, therefore, larger, and the maximum frequency is lower. A similar result was observed in the blunt fin flows. Since L_{sep} on centerline depends primarily on D, it can be held fixed while δ_0 is varied. With $D=1.27$ cm, the maximum value of $N_L(1.1)$ was about 1.3-1.4 kHz for both boundary layers ($\delta_0=0.3$ and 1.6 cm). However, increasing D to 2.54 cm, which increases the physical size of L_{sep} (although L_{sep}/D remains the same) decreased N_L to about 0.9-1 kHz. Robertson found a similar dependence in tests using cylindrical protuberances. In the intermittent region, and in the outer region of separated flow, spectra generated by different cylinders at different flow conditions could be correlated if the power and frequency axes were normalized by $U_\infty q_\infty^2 L_{sep}$ and L_{sep}/U_∞, respectively.

For the fin tests, values of $N_L L_{sep}/U_\infty = 0.06$ and 0.09 were obtained for $D=1.27$ and 2.54 cm, respectively. Values for the ramp flows are 0.09 and 0.11 at stations 1 and 2, respectively. These four values, at a single U_∞, exhibit as much variation as the raw frequency data, so the result is inconclusive. Although for both configurations the maximum value of $N_L(1.1)$ decreases with increasing L_{sep}, more data over a wider range of L_{sep} and at different values of U_∞ are needed before use of $N_L L_{sep}/U_\infty$ as a frequency correlating parameter can be properly evaluated.

Upstream Influence

Experimentally, upstream influence, L_u, is generally estimated from mean wall pressure distributions using the method sketched in Fig. 9a. In absolute terms, it will be

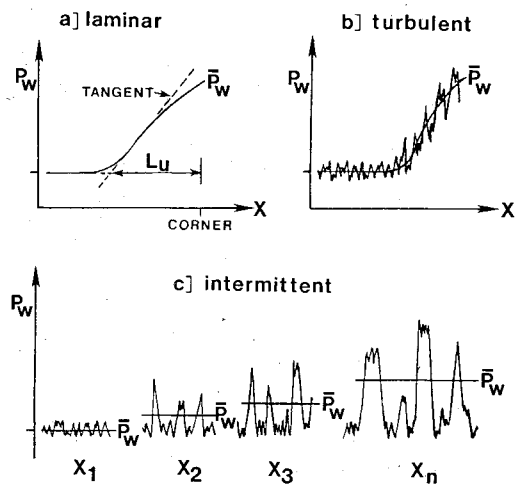

Fig. 9 Physical interpretation of upstream influence.

slightly underestimated, but the method provides consistency within a given test series, and for comparison with other results. Values of 2.4 δ_0 and 2.3 δ_0 at stations 1 and 2 agree well with the correlated data of Ref. 23.

In a steady laminar or turbulent flow, L_u has a clear physical interpretation, as shown in Figs. 9a and b. The wall pressures sketched are those which might be measured at any instant. In turbulent flow, the fluctuation amplitude about the mean increases, but as $\bar{P}_w$ increases with X the signal as a whole moves up the pressure axis. In the intermittent case, a sketch at an instant cannot represent the downstream increase in $\bar{P}_w$. A time history is needed at several stations, say X_1 through X_n, and the mean values at each point connected (Fig. 9c). The point X_0 where $\bar{P}_w$ first increases above $\bar{P}_{w0}$ is not the mean upstream influence. At X_0, γ and the mean shock wave strength are small, but sufficient to increase $\bar{P}_w$ above $\bar{P}_{w0}$. Typically at X_0, $P_w < P_{w0} + 3\sigma p_{w0}$ for about 95% of the time. Thus, X_0 is the furthest upstream station at which the pressure fluctuations due to the unsteady shock structure are large enough and frequent enough to cause a measurable increase in $\bar{P}_w$. Upstream influence is spread over the region defined by L_i, with each point characterized by a value of γ.

Concluding Remarks

Wall pressure fluctuations have been measured in a separated, two-dimensional, compression ramp-induced shock wave turbulent boundary-layer interaction. The test conditions were a nominal freestream Mach number of 3, with Reynolds numbers based on boundary-layer thicknesses of 7.8×10^5 and 1.4×10^6. The wall temperature condition was approximately adiabatic. The measurements show that:

1) Large-amplitude pressure fluctuations exist throughout the interaction, particularly near separation and reattachment.

2) The separation shock wave structure is highly unsteady generating an intermittent wall pressure signal. Mean wall pressures in this region result from the superposition of relatively low-frequency, large-amplitude pressure fluctuations on the pressure signal of the undisturbed turbulent boundary layer. At each station in this region an intermittency factor can be calculated, defining the fraction of time that the flowfield is disturbed.

3) The characteristics of the unsteady separation shock wave structure are similar to those in blunt fin-induced flows. In both flows, the frequencies of the shock motion are of similar magnitude and decrease as the length of the separated flow region increases. The streamwise length scale of the shock wave motion is in both cases a significant fraction of the distance from the interaction start to separation.

4) The unsteadiness causes upstream influence to vary constantly with time. The instantaneous values fall in a band whose length scale is that of the shock structure motion. Conventionally, upstream influence is determined from time-averaged measurements and is defined as the distance from the ramp corner line to the point where the mean wall pressure first exceeds the undisturbed level. This is actually the upstream boundary of the band and is where the shock-induced pressure fluctuations are large enough and frequent enough to cause a measurable increase in the mean wall pressure.

Acknowledgments

This work was supported by the Naval Air Systems Command, Contract N60921-82-K-0064, monitored by Dale Hutchins, and the Air Force Office of Scientific Research, contract F49620-81-K-0018, monitored by Dr. James Wilson.

References

[1] Horstman, C. C. and Hung, C. M., "Computation of Three-Dimensional Turbulent Separated Flows at Supersonic Speeds," AIAA Paper 79-0002, New Orleans, La., Jan. 1979.

[2] Kussoy, M. I., Viegas, J. R., and Horstman, C. C., "Investigation of Three-Dimensonal Shock Wave Separated Boundary Layer," *AIAA Journal*, Vol. 18, Dec. 1980, pp. 1477-1484.

[3] Viegas, J. R. and Horstman, C. C., "Comparison of Multi-Equation Turbulence Models for Several Shock Boundary Layer Interaction Flows," *AIAA Journal*, Vol. 17, Aug. 1979, pp. 811-820.

[4] Bogdonoff, S. M., "Some Experimental Studies of the Separation of Supersonic Turbulent Boundary Layers," Dept. of Aeronautical Engineering, Princeton University, Princeton, N.J., Rept. 336, June 1955.

[5] Kistler, A. L., "Fluctuating Wall Pressure Under a Separated Supersonic Flow," *Journal of the Acoustical Society of America*, Vol. 36, March 1964, pp. 543-550.

[6] Price, A. E. and Stallings, R. L., "Investigation of Turbulent Separated Flows in the Vicinity of Fin Type Protuberances at Supersonic Mach Numbers," NASA TN D-3804, Feb. 1967.

[7] Winkelmann, A. E., "Experimental Investigations of a Fin Protuberance Partially Immersed in a Turbulent Boundary Layer at Mach 5," NOLTR-72-33, Jan. 1972.

[8] Kaufman, L. G., Korkegi, R. H., and Morton, L. C., "Shock Impingement Caused by Boundary Layer Seapration Ahead of Blunt Fins," ARL 72-0118, Aug. 1972.

[9] Robertson, J. E., "Prediction of In-Flight Fluctuating Pressure Environments Including Protuberance Induced Flow," Wyle Laboratories Research Staff Rept. WR71-10, March 1971.

[10] Degrez, G., "Exploratory Experimental Investigation of the Unsteady Aspects of Blunt Fin-Induced Shock Wave Turbulent Boundary Layer Interactions," MSE thesis No. 1516-T, Mechanical and Aerospace Engineering Dept., Princeton University, June 1981.

[11] Dolling, D. S. and Bogdonoff, S. M., "An Experimental Investigation of the Unsteady Behavior of Blunt Fin-Induced Shock Wave Turbulent Boundary Layer Interactions," AIAA Paper 81-1287, June 1981.

[12] Horstman, C. C. and Owen, F. K., "New Diagnostic Technique for the Study of Turbulent Boundary Layer Separation," *AIAA Journal*, Vol. 12, Oct. 1974, pp. 1436-1438.

[13] Coe, C. F., Chyu, W. J., and Dods, J. B., "Pressure Fluctuations Underlying Attached and Separated Supersonic Turbulent Boundary Layers and Shock Waves," AIAA Paper 73-996, Seattle, Wash., Oct. 1973.

[14] Chyu, W. J. and Hanly, R. D., "Power and Cross Spectra and Space-Time Correlations of Surface Fluctuating Pressures at Mach Numbers Between 1.6 and 2.5," NASA TN-D-5440, Sept. 1969.

[15] Settles, G. S., Vas, I. D., and Bogdonoff, S. M., "Details of a Shock Separated Turbulent Boundary Layer at a Compression Corner," *AIAA Journal*, Vol. 14, Dec. 1976, pp. 1709-1715.

[16]Settles, G. S., "An Experimental Study of Compressible Turbulent Boundary Layer Separation at High Reynolds Numbers," Ph.D. Dissertation, Aerospace and Mechanical Sciences Dept., Princeton Univ., Princeton, N.J., Sept. 1975.

[17]Raman, K. R., "A Study of Surface Pressure Fluctuations in Hypersonic Turbulent Boundary Layers," NASA CR-2386, Feb. 1974.

[18]Laganelli, A. L. and Martelluci, A., "Prediction of Turbulent Wall Pressure Fluctuations in Attached Boundary Layer Flow," AIAA Paper 81-1227, June 1981.

[19]Lewis, T. L. and Dods, J. B. Jr., "Wind Tunnel Measurements of Surface-Pressure Fluctuations at Mach Numbers of 1.6, 2.0 and 2.5 Using Twelve Different Transducers," NASA TN-D-7087, Oct. 1972.

[20]Bies, D. A., "A Review of Flight and Wind Tunnel Measurements of Boundary Layer Pressure Fluctuations and Induced Structural Response," NASA CR-626, Oct. 1966.

[21]Settles, G. S. and Teng, H. Y., "Flow Visualization of Separated 3-D Shock Wave/Turbulent Boundary Layer Interations," AIAA Paper 82-0229, Jan. 1982.

[22]Dolling, D. S. and Or, C. T., "Unsteadiness of the Shock Wave Structure in Attached and Separated Compressor Ramp Flow Fields," AIAA Paper 83-1715, July 1983.

[23]Settles, G. S., Perkins, J. J., and Bogdonoff, S. M., "Upstream Influence Scaling of 2-D and 3-D Shock/Turbulent Boundary Layer Interactions at Compression Corners," AIAA Paper 81-0334, Jan. 1981.